

Synthesis, Characterization, and Solution Properties of a Novel Cross-Bridged Cyclam Manganese(IV) Complex Having Two Terminal Hydroxo Ligands

Guochuan Yin,[†] James M. McCormick,[†] Maria Buchalova,[†] Andrew M. Danby,[†] Kent Rodgers,[§] Victor W. Day,[†] Kevyn Smith,[§] Chris M. Perkins,[‡] David Kitko,[‡] John D. Carter,[‡] William M. Scheper,[‡] and Daryle H. Busch^{*†}

Department of Chemistry, The University of Kansas, Lawrence, Kansas 66045,
Department of Chemistry and Molecular Biology, North Dakota State University,
Fargo, North Dakota 58105-5516, and Procter and Gamble, Cincinnati, Ohio 45202

Received December 9, 2005

A novel monomeric tetravalent manganese complex with the cross-bridged cyclam ligand 4,11-dimethyl-1,4,8,11-tetraazabicyclo[6.6.2]hexadecane (Me₂EBC), [Mn^{IV}(Me₂EBC)(OH)₂](PF₆)₂, was synthesized by oxidation of Mn^{II}(Me₂EBC)Cl₂ with H₂O₂ in the presence of NH₄PF₆ in aqueous solution. The X-ray crystal structure determination of this manganese(IV) compound revealed that it contains two rare terminal hydroxo ligands. EPR studies in dry acetonitrile at 77 K show two broad resonances at $g = 1.96$ and 3.41 , indicating that the manganese(IV) exists as a high-spin d³ species. Resonance Raman (rR) spectra of this manganese(IV) species reveal that the dihydroxy moiety, Mn^{IV}-(OH)₂, is also the dominant species in aqueous solution (pH < 7). pH titration provides two pK_a values, 6.86(4) and 10.0(1), associated with stepwise removal of the last two oxygen-bound protons from [Mn^{IV}(Me₂EBC)(OH)₂]²⁺. The cyclic voltammetry of this manganese(IV) complex in dry acetonitrile at 298 K demonstrates two reversible redox processes at +0.756 and -0.696 V (versus SHE) for the Mn⁴⁺/Mn³⁺ and Mn³⁺/Mn²⁺ couples, respectively. This manganese(IV) complex is relatively stable in weak acidic aqueous solution but easily degrades in basic solution to manganese(III) derivatives with an 88 ± 1% yield.

Introduction

The element manganese shares an essential role in electron- and oxygen-transfer processes in nature with iron and copper. Further, manganese-containing enzymes are involved in a number of fundamental biological oxidation–reduction processes, including delignification,¹ superoxide dismutation,² and oxygen evolution.³ High oxidation state manganese moieties have long been accepted as the reactive intermediates in the corresponding reactions such as water

oxidation for oxygen evolution. Oxo-manganese(V) reactive units (LMn^V=O) are believed to serve as the key intermediates in oxygenations mediated by synthetic manganese complexes,⁴ while in Photosystem II, the presence of the mixed valence bis(μ -oxo)dimanganese(III/IV) groups have long been discussed, first as linked pairs of dimers, and most recently as a cubane-like trimer linked to a monomer.³ To understand the mechanisms mediated by these manganese systems and for potential industrial applications, various mimics and models have been explored, and those studies

* To whom correspondence should be addressed. E-mail: busch@ku.edu.

[†] The University of Kansas.

[§] North Dakota State University.

[‡] Procter and Gamble.

- (1) (a) Paice, M. G.; Bourbonnais, R.; Reid, I. D.; Archibald, F. S.; Jurasek, L. *J. Pulp Pap. Sci.* **1995**, *21*, J280. (b) Mtui, G.; Nakamura, Y. *J. Chem. Eng. Jpn.* **2004**, *37*, 113. (c) Reddy C. A. *J. Biotechnol.* **1993**, *30*, 91. (d) Hofrichter, M. *Enzyme Microb. Technol.* **2002**, *30*, 454.
- (2) (a) Michelson, J. M.; McCord, J. M.; Fridovich, I., Eds. *Superoxide and Superoxide Dismutases*; Academic: New York, 1977. (b) Bull, C.; Niederhoffer, E. C.; Yoshida, T.; Fee, J. A. *J. Am. Chem. Soc.* **1991**, *113*, 4069. (c) Kachadourian, R.; Batinic-Haberle, I.; Fridovich, I. *Inorg. Chem.* **1999**, *38*, 391.

- (3) (a) Mukhopadhyay, S.; Mandal, S. K.; Bhaduri, S.; Armstrong, W. H. *Chem. Rev.* **2004**, *104*, 3981. (b) Yachandra, V. K.; Sauer, K.; Klein, M. P. *Chem. Rev.* **1996**, *96*, 2927. (c) Tommos, C.; Babcock, G. T. *Acc. Chem. Res.* **1998**, *31*, 18. (c) Ferreira, K. N.; Iverson, T. M.; Maghlaoui, K.; Barber, J.; Iwata, S. *Science* **2004**, *303*, 1831.
- (4) (a) Adam, W.; Roschmann, K. J.; Saha-Möllner, C. R.; Seebach, D. *J. Am. Chem. Soc.* **2002**, *124*, 5068. (b) Finney, N. S.; Pospisil, P. J.; Chang, S.; Palucki, M.; Konsler, R. G.; Hansen, K. B.; Jacobsen, E. N. *Angew. Chem., Int. Ed. Engl.* **1997**, *36*, 1720. (c) Meunier, B.; Guilmet, E.; De Carvalho, M.; Poilblanc, R. *J. Am. Chem. Soc.* **2000**, *122*, 2675. (d) Battioni, P.; Renaud, J. P.; Bartoli, J. F.; Reina-Arilles, M.; Fort, M.; Mansuy, D. *J. Am. Chem. Soc.* **1988**, *110*, 8462.

have provided much mechanistic information.^{4a,c,d,5} The practice of synthesizing high oxidation state manganese biomimics rises above all other experimental protocols used in these mechanism studies because the high oxidation state manganese compounds have the potential of directly elucidating the reaction mechanism. Indeed, the literature reports a progression of mononuclear, dinuclear, trinuclear, and tetranuclear compounds of manganese(IV) or mixed valence manganese(IV, III, and II) that have been designed and synthesized in the mission to reveal the mechanism of oxygen evolution by Photosystem II.^{3,6} Probably because of the high redox potential of the Mn(V/IV) couple and the poor stability of manganese(V) oxo porphyrins, there has, until now, been no report of well-characterized heme-containing manganese(V) oxo (i.e., $\text{Mn}^{\text{V}}=\text{O}$) derivatives, although nitrido manganese(V) complexes with porphyrin ligands have been well characterized.⁷ This is true despite generally accepted reports of the detection in solution of oxo-manganese(V) species and their assignment as the key active intermediates in oxygenation reactions mediated by heme-containing manganese complexes. Several oxo-manganese(V) complexes with other synthetic ligands have been successfully isolated from solution and characterized. These Mn(V) derivatives are capable of transferring oxygen to easily oxidized substrates, such as triphenylphosphine, but not to common olefinic double bonds. The obvious conclusion is that the manganese(V) derivatives that are relatively easy to isolate have low reactivities.⁸ In a few cases, synthetic heme-containing oxo-manganese(IV) species have been proposed as active intermediates for oxygen transfer and a few these oxo-manganese(IV) compounds have been successfully isolated.⁹

In these model compounds, the main ligand plays a critical role in determining the stability and catalytic efficiency of metal complexes. Porphyrin derivatives, salen derivatives, and polyamine derivatives are commonly selected as ligands for biomimetic studies, such as mimicking heme-containing

enzymes, homogeneous catalysis, and the reactive center involved in Photosystem II. For applications in aqueous solution (e.g., catalytic water oxidation), polyamine derivatives are favored over other derivatives because of their solubility and availability.³ Resistance of the complex to ligand dissociation is always a major concern in matters of catalyst efficacy. The ultra-rigid trans-cross-bridged tetraazamacrocyclic derivatives described here are outstanding among polyamine derivatives because of the exceptional kinetic stabilities of their metal complexes.¹⁰

The bridging group in these trans-bridged macrocyclic ligands, such as 4,11-dimethyl-1,4,8,11-tetraazabicyclo[6.6.2]-hexadecane (Me_2EBC), constitutes a constraint that limits the library of conformations accessible to the ligand, and those eliminated conformations include sets that provide the simplest pathways to ligand dissociation.¹⁰ This design feature has been exploited to produce a family of manganese complexes that are highly selective oxidation catalysts.^{10c,11} In many applications, the durability in service of catalysts is a determining factor in their implementation. The extension of service lifetime that these catalysts gain from the constraining cross-bridge has led to their consideration in a number of applications.¹² The second property in which these particular catalysts excel is their selectivity in catalytic oxidation processes. Unlike the more familiar catalysts based on porphyrin ligands,^{4,5,13} the highest oxidation state achieved by manganese in these systems is +4, and as discussed below, $[\text{Mn}^{\text{IV}}(\text{Me}_2\text{EBC})(\text{OH})_2]^{2+}$ is, under appropriate conditions, a very moderate oxidizing agent. To understand the physical chemistry properties and chemical reactivities of these exciting manganese complexes with the cross-bridged macrocyclic ligands, the corresponding complexes of divalent and trivalent manganese have been studied in detail, and their chemistries have been summarized in earlier publications.^{10c,11} Those previous studies reveal that the manganese complexes of Me_2EBC are capable of withstanding harsh aqueous conditions without decomposing or dimerizing, and catalytic studies with $\text{Mn}^{\text{II}}(\text{Me}_2\text{EBC})\text{Cl}_2$ have already displayed its

- (5) (a) Arassasingham, R. D.; He, G. X.; Bruce, T. C. *J. Am. Chem. Soc.* **1993**, *115*, 7985. (b) Groves, J. T.; Lee, J.; Marla, S. S. *J. Am. Chem. Soc.* **1997**, *119*, 6269.
- (6) (a) Chan, M. K.; Armstrong, W. A. *Inorg. Chem.* **1989**, *28*, 3779. (b) Caudle, M. T.; Kampf, J. W.; Kirk, M. L.; Rasmussen, P. G.; Pecoraro, V. L. *J. Am. Chem. Soc.* **1997**, *119*, 9297. (c) Visser, H.; Dubé, C. E.; Armstrong, W. H.; Sauer, K.; Yachandra, V. K. *J. Am. Chem. Soc.* **2002**, *124*, 11008. (d) Wieghardt, K.; Bossek, U.; Nuber, B.; Weiss, J.; Bonvoisin, J.; Corbella, M.; Vitols, S. E.; Girerd, J. J. *J. Am. Chem. Soc.* **1988**, *110*, 7398. (e) Pavacik, P. S.; Huffman, J. C.; Christou, G. *J. Chem. Soc., Chem. Comm.* **1986**, 43. (f) Magers, K. D.; Smith, C. G.; Sawyer, D. T. *Inorg. Chem.* **1980**, *19*, 492.
- (7) (a) Hill, C. L.; Hollander, F. J. *J. Am. Chem. Soc.* **1982**, *104*, 7318. (b) Buchler, J. W.; Dreher, C.; Lay, K. L.; Lee, Y. J.; Scheidt, W. R. *Inorg. Chem.* **1983**, *22*, 888.
- (8) (a) Collins, T. J.; Powell, R. D.; Slebodnick, C.; Uffelman, E. S. *J. Am. Chem. Soc.* **1990**, *112*, 899. (b) Collins, T. J.; Gordon-Wylie, S. W. *J. Am. Chem. Soc.* **1989**, *111*, 4511. (c) MacDonnell, F. M.; Fackler, N. L. P.; Stern, C.; O'Halloran, T. V. *J. Am. Chem. Soc.* **1994**, *116*, 7431. (d) Mandimutsira, B.; Ramdhanie, B.; Todd, R. C.; Wang, H.; Zareba, A. A.; Czernuszewicz, R. S.; Goldberg, D. P. *J. Am. Chem. Soc.* **2002**, *124*, 15170. (e) Wang, H.; Mandimutsira, B.; Todd, R. C.; Ramdhanie, B.; Fox, J. P.; Goldberg, D. P. *J. Am. Chem. Soc.* **2004**, *126*, 18.
- (9) (a) Schardt, B. C.; Hollander, F. J.; Hill, C. L. *J. Am. Chem. Soc.* **1982**, *104*, 3694. (b) Camenzind, M. J.; Hollander, F. J.; Hill, C. L. *Inorg. Chem.* **1983**, *22*, 3776. (c) Groves, J. T.; Stern, M. K. *J. Am. Chem. Soc.* **1988**, *110*, 8628.

- (10) (a) Cagginess, D. K.; Margerum, D. W. *J. Am. Chem. Soc.* **1970**, *92*, 2151. (b) Hubin, T. J.; McCormick, J. M.; Collinson, S. R.; Busch, D. H.; Alcock, N. W. *J. Chem. Soc., Chem. Comm.* **1998**, 1675. (c) Hubin, T. J.; McCormick, J. M.; Collinson, S. R.; Buchalova, M.; Perkins, C. M.; Alcock, N. W.; Kahol, P. K.; Raghunathan, A.; Busch, D. H. *J. Am. Chem. Soc.* **2000**, *122*, 2512. (d) Niu, W.; Wong, E. H.; Weisman, G. R.; Hill, D. C.; Tranchemontagne, D. J.; Lam, K.; Sommer, R. D.; Zakharov, L. N.; Rheingold, A. L. *Dalton Trans.* **2004**, *21*, 3536.
- (11) (a) Hubin, T. J.; McCormick, J. M.; Alcock, N. W.; Busch, D. H. *Inorg. Chem.* **2001**, *40*, 435. (b) Hubin, T. J.; McCormick, J. M.; Collinson, S. R.; Alcock, N. W.; Clase, H. J.; Busch, D. H. *Inorg. Chim. Acta* **2003**, *346*, 76. (c) Collinson, S. R.; Alcock, N. W.; Hubin, T. J.; Busch, D. H. *J. Coord. Chem.* **2001**, *52* (4), 317. (d) Collinson, S. R.; Alcock, N. W.; Raghunathan, A.; Kahol, P. K.; Busch, D. H. *Inorg. Chem.* **2000**, *39* (4), 757. (e) Hubin, T. J. Ph.D. Dissertation, The University of Kansas, Lawrence, KS, 1998.
- (12) (a) Busch, D. H.; Collinson, S. R.; Hubin, T. J.; Labeque, R.; Williams, B. K.; Johnston, J. P.; Kitko, D. J.; Burekett—St. Laurent, J. C. T. R.; Perkins, C. M. Bleach Compositions Containing Metal Bleach Catalyst for Detergents. International Patent WO 98/39406, 1998. (b) Busch, D. H.; Collinson, S. R.; Hubin, T. J. Catalysts and Methods for Catalytic Oxidation. International Patent WO98/39098, 1998.
- (13) (a) Groves, J. T. *J. Chem. Res.* **1985**, 62, 928. (b) Garrison, J. M.; Bruce, T. C. *J. Am. Chem. Soc.* **1989**, *111*, 191. (c) Newcomb, M.; Shen, R.; Choi, S.; Toy, P. H.; Hollenberg, P. F.; Vaz, A. D. N.; Coon, M. J. *J. Am. Chem. Soc.* **2000**, *122*, 2677.

excellent robustness in the course of hydrogen abstraction and oxygen-transfer processes.^{10c} A mononuclear manganese(III) complex with a rare OH ligand, $[\text{Mn}^{\text{III}}(\text{Me}_2\text{EBC})(\text{OH})(\text{OAc})](\text{PF}_6)$, was also isolated and characterized, including an X-ray structure determination.^{11a} Because of their value in elucidating the key active intermediates in reactions catalyzed by these manganese complexes, such as hydrogen abstraction and oxygen transfer, synthesis of high oxidation state manganese complexes, for example manganese(IV), should be explored. Here, we report the synthesis and structure of the corresponding novel manganese(IV) compound with two hydroxo ligands and discuss its oxidation–reduction and acid–base properties. The structure has been confirmed in both the solid state and in solution. Also the EPR, $\text{p}K_{\text{a}}$, and electrochemistry contribute to the clear understanding of this rare dihydroxy complex of manganese(IV). The properties of the compound provide insight into its behavior as a catalyst. $[\text{Mn}^{\text{IV}}(\text{Me}_2\text{EBC})(\text{OH})_2](\text{PF}_6)_2$ is conveniently synthesized by oxidation of $\text{Mn}^{\text{II}}(\text{Me}_2\text{EBC})\text{Cl}_2$ with hydrogen peroxide in the presence of NH_4PF_6 in aqueous solution.

Although many manganese(IV) complexes containing Mn–O bonds have been isolated and well-characterized, most of the oxygen ligands are organic groups such as phenoxide or methyloxy, bridging μ -O, and μ -OH, or terminal hydroxo groups in multinuclear manganese complexes.^{3a,6d,14} Because manganese complexes with terminal hydroxo ligands are usually found in multinuclear oxo-bridged clusters, monomeric manganese complexes with the terminal hydroxo ligand are very rare and even then limited to lower oxidation states (i.e., manganese(II) and manganese(III)), examples of which have been characterized.^{11a,15} To our knowledge, the compound reported here, $[\text{Mn}^{\text{IV}}(\text{Me}_2\text{EBC})(\text{OH})_2](\text{PF}_6)_2$, is the first monomeric manganese(IV) complex with the terminal hydroxo ligands to be isolated and thoroughly characterized.¹⁶ Indeed, such pure compounds with this rare structural feature must be of considerable importance in confronting the mechanistic issues described above, including catalytic activity, water oxidation, and O_2 evolution.

Experimental Section

$\text{Mn}^{\text{II}}(\text{Me}_2\text{EBC})\text{Cl}_2$ (+99.9%) was generously supplied by the Procter and Gamble Company. Other reagents were purchased from Aldrich or Lancaster. Elemental analysis was performed by Quantitative Technologies, Inc.

- (14) (a) Caudle, M. T.; Pecoraro, V. L. *J. Am. Chem. Soc.* **1997**, *119*, 3415. (b) Pal, S.; Chan, M. K.; Armstrong, W. H. *J. Am. Chem. Soc.* **1992**, *114*, 6398. (c) Pal, S.; Armstrong, W. H. *Inorg. Chem.* **1992**, *31*, 5417. (d) Carrell, T. G.; Bourles, E.; Lin, M.; Dismukes, G. C. *Inorg. Chem.* **2003**, *42*, 2849.
- (15) (a) Gupta, R.; MacBeth, C. E.; Young, V. G., Jr.; Borovik, A. S. *J. Am. Chem. Soc.* **2002**, *124*, 1136. (b) MacBeth, C. E.; Gupta, R.; Mitchell-Koch, K. R.; Young, V. G., Jr.; Lushington, G. H.; Thompson, W. H.; Hendrich, M. P.; Borovik, A. S. *J. Am. Chem. Soc.* **2004**, *126*, 2556. (c) Shirin, Z.; Hammes, B. S.; Young, V. G., Jr.; Borovik, A. S. *J. Am. Chem. Soc.* **2000**, *122*, 1836. (d) Shirin, Z.; Young, V. G., Jr.; Borovik, A. S. *J. Chem. Soc. Chem. Commun.* **1997**, 1967. (e) Eichhorn, D. M.; Armstrong, W. H. *J. Chem. Soc., Chem. Commun.* **1992**, 85.
- (16) There was one manganese(IV) complex with a terminal hydroxo ligand reported in 1967, but no crystal data was available to confirm the structure (Poddar, S. N.; Podder, N. G. *Indian J. Chem.* **1968**, *6*, 276).

Physical Measurements. Mass spectra were measured by the Analytical Service of the University of Kansas on a VG ZAB HS spectrometer equipped with a xenon gun. Electrochemical experiments were performed under nitrogen in dry acetonitrile on a CH Instruments Model 620A using a locally constructed cell. A Pt button was used as the working electrode in conjunction with a Pt-wire counter electrode and an Ag/Ag^+ nonaqueous electrode was used as the reference electrode. Tetrabutylammonium hexafluorophosphate (0.1 M) was the supporting electrolyte in all cases.

Potentiometric titrations were performed under N_2 at 25.0 °C with an ionic strength of 0.1000 (KNO_3) on a Brinkmann Metrohm 736GP Titrino equipped with a Brinkmann combination electrode. In a typical titration, ~ 10 mg of $[\text{Mn}(\text{Me}_2\text{EBC})(\text{OH})_2](\text{PF}_6)_2 \cdot \text{H}_2\text{O}$ was placed in 50.0 mL of the supporting electrolyte solution and ~ 2 mL of a standard HNO_3 solution was added to a $\text{pH} < \sim 3$. The resulting solution was titrated to a pH value between 11 and 12. The data were fit using the program HYPERQUAD.

EPR spectra were recorded on a Bruker ESP300E spectrometer operating in the X-band using ~ 1 mM complex in dry CH_3CN at 77 K. Electronic spectra were recorded using a Cary 3 spectrometer controlled by a Dell Dimension XPS P133s computer.

Resonance Raman spectra were excited using 413.1 nm emission from a Kr^+ laser. Samples were contained in a spinning 5 mm NMR tube. Scattered light was collected in the 135° backscattering geometry using an f1 lens. Rayleigh scattering used a holographic notch filter, and the Raman scattered light was focused on the entrance slit of a 0.7 m spectrograph fitted with a 2400 g/mm grating and a LN_2 -cooled CCD camera. Spectral calibration was based on the Raman bands of toluene and dibromomethane. Data were processed and plotted using standard software.

Synthesis of $[\text{Mn}^{\text{IV}}(\text{Me}_2\text{EBC})(\text{OH})_2](\text{PF}_6)_2 \cdot \text{H}_2\text{O}$. A 10 mL aqueous solution containing 0.38 g (0.001 mol) of $\text{Mn}^{\text{II}}(\text{Me}_2\text{EBC})\text{Cl}_2$ and 0.815 g (0.005 mol) of NH_4PF_6 was prepared. Two milliliters of 30% H_2O_2 was added stepwise, with stirring, to the prepared solution over a period of 1 h. A deep-purple solution formed immediately. Stirring of the reaction solution was continued until bubbles no longer formed in the solution (about 1 h). During this time, a purple precipitate gradually separated. The resulting reaction mixture was stored in a freezer overnight. The purple precipitate was filtered with a glass frit and washed with H_2O . The product was collected and dried overnight under reduced pressure at room temperature. About 0.31 g of crude product was obtained as a purple powder. To recrystallize the crude product, it was completely dissolved in water. Then, an aqueous solution saturated with 1 g of NH_4PF_6 was added to the solution with stirring. A purple precipitate gradually formed. After it was filtered and dried under reduced pressure at room temperature, about 0.2 g of product was obtained. Yield: 30%. Anal. Calcd for $\text{MnC}_{14}\text{H}_{34}\text{N}_4\text{O}_3\text{P}_2\text{F}_{12}$: C, 25.81; H, 5.22; N, 8.60; F, 35.02; Mn, 8.43%. Found: C, 25.76; H, 5.07; N, 8.51; F, 35.76; Mn, 8.28%. The ESI positive mass spectrum in acetone (NBA matrix) exhibited a peak at $m/z = 342$ for $[\text{Mn}(\text{Me}_2\text{EBC})(\text{O})(\text{OH})]^+$. The X-ray quality crystal of the $[\text{Mn}^{\text{IV}}(\text{Me}_2\text{EBC})(\text{OH})_2](\text{PF}_6)_2$ was obtained by evaporation of an aqueous solution containing $[\text{Mn}^{\text{IV}}(\text{Me}_2\text{EBC})(\text{OH})_2](\text{PF}_6)_2$ in the presence of NH_4PF_6 under reduced pressure at room temperature.

Instability of $[\text{Mn}^{\text{IV}}(\text{Me}_2\text{EBC})(\text{OH})_2](\text{PF}_6)_2 \cdot \text{H}_2\text{O}$ in Basic Aqueous Solutions. A saturated aqueous solution containing 0.415 g (0.64 mmol) of $[\text{Mn}^{\text{IV}}(\text{Me}_2\text{EBC})(\text{OH})_2](\text{PF}_6)_2$ was prepared. The pH value of the above solution was adjusted to ~ 10.9 with 2 N NaOH ; then, the solution was stirred at room temperature for 3 days. During this period, the color of the solution changed gradually from purple to red-brown. The final pH value of this solution was ~ 8.3 . After the resulting solution was filtered, the concentration

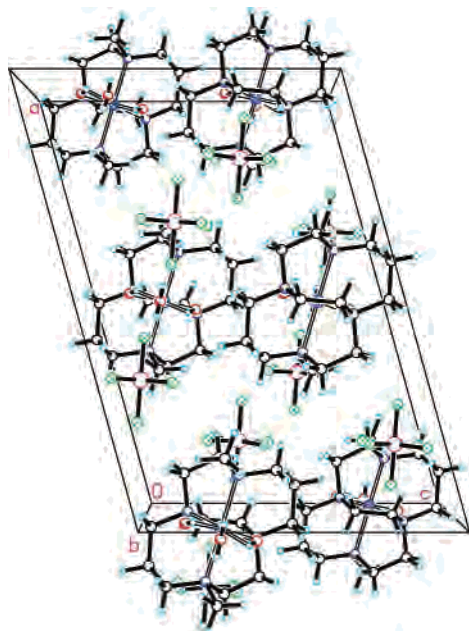


Figure 1. Packing diagram for $[\text{Mn}^{\text{IV}}(\text{Me}_2\text{EBC})(\text{OH})_2](\text{PF}_6)_2 \cdot \text{H}_2\text{O}$.

of the resulting $\text{Mn}^{\text{III}}(\text{Me}_2\text{EBC})$ species in the clean solution was measured with UV–vis spectroscopy and compared with the standard $[\text{Mn}^{\text{III}}(\text{Me}_2\text{EBC})\text{Cl}_2]\text{PF}_6$ sample in the basic medium. Yield of $\text{Mn}^{\text{III}}(\text{Me}_2\text{EBC})$ species based on the initial $[\text{Mn}^{\text{IV}}(\text{Me}_2\text{EBC})(\text{OH})_2](\text{PF}_6)_2$: $88 \pm 1\%$. The dark precipitates were washed with water a few times; then, they were dried in vacuo. This dark precipitate was not combustible in air. Yield: $8.9 \pm 0.4\%$ (based on MnO_2).

Crystal Structure Analysis. A red prism-shaped crystal of dimensions $0.38 \times 0.26 \times 0.14$ mm was selected for X-ray structural analysis. Intensity data for this compound were collected using a Bruker APEX CCD area detector¹ mounted on a Bruker D8 goniometer using graphite-monochromated Mo $K\alpha$ radiation ($\lambda = 0.71073$ Å). The data were collected at 100(2) K. The intensity data were measured as a series of ω oscillation frames each of 0.25° for 10 s/frame. The centrosymmetric monoclinic space group $C2/c$ was determined by systematic absences and statistical tests and verified by subsequent refinement. The structure was solved by direct methods and refined by full-matrix least-squares methods on F^2 .³ All hydrogen atoms were located from a difference Fourier synthesis and included in the structural model as individual isotropic atoms whose parameters were allowed to vary during least-squares refinement cycles. The final structural model incorporated anisotropic thermal parameters for all non-hydrogen atoms and isotropic thermal parameters for all hydrogen atoms.

Results and Discussion

Solid State Structure of the Manganese(IV) Complex.

X-ray quality crystals of $[\text{Mn}^{\text{IV}}(\text{Me}_2\text{EBC})(\text{OH})_2](\text{PF}_6)_2 \cdot \text{H}_2\text{O}$ were isolated by evaporating an aqueous solution of $\text{Mn}^{\text{IV}}(\text{Me}_2\text{EBC})(\text{OH})_2^{2+}$ in the presence of NH_4PF_6 under reduced pressure at room temperature. A packing diagram for the $\text{Mn}^{\text{IV}}(\text{Me}_2\text{EBC})(\text{OH})_2^{2+}$ salt is shown in Figure 1. The Mn atom of the cation and the oxygen atom for the water solvent molecule of crystallization are located on the crystallographic C_2 axis at $(1/2, y, 3/4)$ in the unit cell. The crystallographically unique PF_6^- group is disordered and was modeled using three different orientations with refined occupancies of 0.363(4),

Table 1. Crystal Data and Structure Refinement

empirical formula	$(\text{C}_{14}\text{H}_{32}\text{MnN}_4\text{O}_2)^{2+} (\text{PF}_6)_2^- (\text{H}_2\text{O})$ $\text{C}_{14}\text{H}_{34}\text{F}_{12}\text{MnN}_4\text{O}_3\text{P}_2$
fw	651.33
crystal system	monoclinic
space group	$C2/c$
unit cell dimensions	$a = 17.939(1)$ Å, $\alpha = 90.000^\circ$ $b = 11.656(1)$ Å, $\beta = 105.465(2)^\circ$ $c = 12.292(1)$ Å, $\gamma = 90.000^\circ$
vol	$2477.3(3)$ Å ³
Z	4
density (calcd)	1.746 Mg/m ³
wavelength	0.71073 Å
temp	$100(2)$ K
$F(000)$	1332
abs coeff	0.778 mm ⁻¹
abs correction	semiempirical from equivalents
max and min transmission	0.899 and 0.757
θ range for data collection	2.11 – 30.51°
reflns collected	10 089
independent reflns	3697 [$R_{\text{int}} = 0.024$]
data/restraints/params	3697/916/343
wR2 ^a (F^2 all data)	$\text{wR2} = 0.149$
R1 ^b (F obsd data)	$R1 = 0.064$
GOF on F^2	1.305
obsd data [$I > 2\sigma(I)$]	3621
largest and mean shift (s.u.)	0.001 and 0.000
largest diff peak and hole	0.96 and -0.51 e/Å ³

$$^a \text{wR2} = \{[\sum(w(F_o^2 - F_c^2)^2)/\sum(w(F_o^2)^2)]^{1/2}, ^b R1 = \sum||F_o| - |F_c||/\sum|F_o|.$$

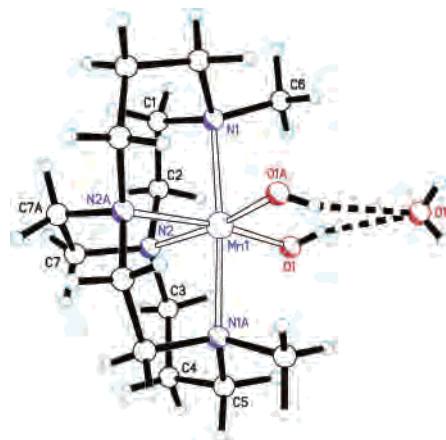


Figure 2. Solid-state structure of $\text{Mn}^{\text{IV}}(\text{Me}_2\text{EBC})(\text{OH})_2 \cdot \text{H}_2\text{O}$ (data in Table 1 and bond lengths and angles in Table 2).

0.318(8), and 0.318(8) for the unprimed, primed, and double-primed fluorines, respectively. The crystal data and structure refinement results for the complex are given in Table 1. Figure 2 shows the structure of the six-coordinate $\text{Mn}^{\text{IV}}(\text{Me}_2\text{EBC})(\text{OH})_2^{2+}$ dication hydrogen-bonded to the water solvent molecule of crystallization. As expected on the basis of the previously published structures of the $\text{Mn}^{\text{II}}(\text{Me}_2\text{EBC})^{2+}$ and $\text{Mn}^{\text{III}}(\text{Me}_2\text{EBC})^{3+}$ complexes,^{9c,10a} the four nitrogen donors of the cross-bridged tetraazamacrocyclic ligands occupy four contiguous coordination sites of the pseudo-octahedral Mn^{IV} coordination sphere, and the two monodentate hydroxo ligands occupy the remaining pair of cis sites.

These two hydroxo ligands are hydrogen-bonded in the crystal to the water solvent molecule of crystallization; the hydroxo and water protons were located from a difference Fourier technique and included in the structural model as independent isotropic atoms whose parameters were allowed to vary in the least-squares refinement cycles. Selected bond

Table 2. Selected Bond Distances (Å) and Angles (deg) for the Mn^{IV}(Me₂EBC)(OH)₂²⁺ Cation^a

[Mn ^{IV} (Me ₂ EBC)(OH) ₂](PF ₆) ₂					
Mn(1)–N(1)	2.110(3)	N(2)–Mn(1)–N(2A)	84.4(1)	O(1)–Mn(1)–N(1)	93.6(1)
Mn(1)–N(2)	2.090(2)	N(2)–Mn(1)–N(1A)	91.0(1)	O(1)–Mn(1)–N(2)	89.2(1)
Mn(1)–O(1)	1.811(2)	N(2A)–Mn(1)–N(1A)	85.8(1)	O(1)–Mn(1)–N(2A)	171.9(1)
O(1)···O(1W)	2.811(4)	N(1A)–Mn(1)–N(1)	175.7(1)	O(1)–Mn(1)–N(1A)	89.3(1)
				O(1)–Mn(1)–O(1A)	97.6(2)
Mn ^{II} (Me ₂ EBC)Cl ₂					
Mn(1)–N(3)	2.325(4)	N(3)–Mn(1)–N(2)	79.5(1) ^{II}	N(4)–Mn(1)–Cl(3)	99.9(1)
Mn(1)–N(1)	2.347(4)	N(3)–Mn(1)–N(4)	158.0(2)	N(1)–Mn(1)–Cl(3)	93.6(1)
Mn(1)–N(2)	2.332(4)	N(2)–Mn(1)–N(4)	83.5(1)	N(3)–Mn(1)–Cl(2)	100.1(1)
Mn(1)–N(4)	2.333(4)	N(3)–Mn(1)–N(1)	83.2(1)	N(2)–Mn(1)–Cl(2)	92.4(1)
Mn(1)–Cl(3)	2.455(2)	N(2)–Mn(1)–N(1)	75.6(2)	N(4)–Mn(1)–Cl(2)	94.4(1)
Mn(1)–Cl(2)	2.456(2)	N(4)–Mn(1)–N(1)	79.2(2)	N(1)–Mn(1)–Cl(2)	166.9(1)
		N(3)–Mn(1)–Cl(3)	94.2(1)	Cl(3)–Mn(1)–Cl(2)	98.9(1)
		N(2)–Mn(1)–Cl(3)	167.9(1)		
[Mn ^{III} (Me ₂ EBC)Cl ₂] ₂ PF ₆					
Mn(1)–N(1)	2.115(4)	N(1)–Mn(1)–N(8)	81.7(2)	N(4)–Mn(1)–Cl(1)	90.6(2)
Mn(1)–N(11)	2.261(6)	N(1)–Mn(1)–N(4)	82.4(2)	N(11)–Mn(1)–Cl(1)	95.2(2)
Mn(1)–N(8)	2.199(5)	N(8)–Mn(1)–N(4)	90.4(2)	N(1)–Mn(1)–Cl(2)	93.1(2)
Mn(1)–N(4)	2.229(6)	N(1)–Mn(1)–N(11)	90.9(2)	N(8)–Mn(1)–Cl(2)	170.6(2)
Mn(1)–Cl(1)	2.269(2)	N(8)–Mn(1)–N(11)	81.4(2)	N(4)–Mn(1)–Cl(2)	96.7(2)
Mn(1)–Cl(2)	2.327(2)	N(4)–Mn(1)–N(11)	170.1(2)	N(11)–Mn(1)–Cl(2)	90.9(2)
		N(1)–Mn(1)–Cl(1)	170.1(1)	Cl(1)–Mn(1)–Cl(2)	94.6(1)
		N(8)–Mn(1)–Cl(1)	91.4(2)		

^a Atoms labeled with an A are related to those labeled without an A by the crystallographic C₂ axis which passes through the Mn atom and the oxygen [O(1W)] of the water molecule of crystallization.

lengths and angles for Mn^{IV}(Me₂EBC)(OH)₂²⁺ are compared with corresponding data for [Mn^{II}(Me₂EBC)Cl₂] and [Mn^{III}(Me₂EBC)Cl₂]₂[PF₆] in Table 2. The general trends for the average Mn–N and Mn–Cl bond lengths in Table 2 are the ones expected from the ionic radii, Mn⁴⁺ < Mn³⁺ < Mn²⁺; direct comparisons can, however, only be made for the high-spin Mn²⁺ and Mn⁴⁺ complexes since Mn³⁺ may experience Jahn–Teller distortion. The ease with which the cross-bridged tetraazamacrocycle encompasses the metal decreases with cation size and is manifested by the cis and trans N–M–N bond angles. The N_{ax}–M–N_{ax} angles decrease in the following order: 175.7(1)° for Mn(IV), 170.1(2)° for Mn(III), and 158.0(2)° for Mn(II). The N_{eq}–M–N_{eq} bond angles decrease in the same order: 84.4(1)° for Mn(IV), 81.7(2)° for Mn(III), and 75.6(2)° for Mn(II).

The 1.811(2) Å Mn–O bond distance and the ability to locate and successfully refine the parameters for the hydroxo and water protons clearly establish the presence of Mn^{IV}–OH moieties. The presence of a hydroxide ligand is also clearly indicated by the bond-valence sum (BVS) of 0.85 for the 1.811(2) Å Mn–O bond and a bond-valence sum of approximately 0.18 for the 2.811(4) Å O1(hydroxide)···O1W(water) hydrogen bond donor–acceptor separation. The hydroxides are the only ligands with the potential for π -bonding to the metal, and they may stabilize the tetravalent state of manganese in this family of compounds sufficiently to moderate the Mn(IV/III) couple, especially in mildly acidic aqueous media (see below). Although a Mn–O bond length of 1.811(2) Å would seem to preclude significant π -bonding in the solid-state, both Mn–O bonds are elongated in the crystal because of hydrogen-bond formation with the water molecule.

The Mn^{IV}–O bonds in [Mn^{IV}(Me₂EBC)(OH)₂](PF₆)₂·H₂O are slightly shorter than the octahedral 1.830(4) Å Mn^{IV}–OH bond in trinuclear [Mn^{IV}₃O₄(OH)(bepa)₃]³⁺ (bepa is *N,N*-

bis(2-pyridylmethyl)ethylamine)^{14b} and much longer than the 1.558(4) Å Mn^V=O bond in a 5-coordinate manganese(V) complex of 1,2-bis(2,2-diphenyl-2-hydroxyethanamido)-benzene.^{8c,15c} The Mn^{IV}–O bonds in [Mn^{IV}(Me₂EBC)(OH)₂](PF₆)₂·H₂O are longer than the 1.771(4) Å average for the Mn^{III}=O bonds in 5-coordinate [Mn^{III}(H₃L)(O)]²⁻ (H₃L = [(tris(*N'*-*tert*-butylureayl)-*N*-ethyl)]amine) and shorter than the 1.873(2) Å average for the Mn^{III}–OH bonds in the corresponding 5-coordinate [Mn^{III}(H₃L)(OH)]⁻: the coordinated O²⁻ and OH⁻ ligands in both of these 5-coordinate complexes are hydrogen bonded to urea nitrogens of the H₃L ligand. The Mn^{IV}–O bonds in [Mn^{IV}(Me₂EBC)(OH)₂](PF₆)₂·H₂O are also much shorter than the 2.059(2) Å Mn^{II}–O bond in Mn^{II}(H₃L)(OH)⁻.^{15a,15c}

A related issue is the failure of the complexes of Me₂-EBC to form μ -O-bridged dimers or oligomers, a behavior of much generality among trivalent and tetravalent manganese complexes, as noted above. The answer is apparent from studies by Borovik and co-workers and the detailed structures of the Me₂EBC complexes. Borovik et al. developed a novel tripodal ligand, [(tris(*N'*-*tert*-butylureayl)-*N*-ethyl)]amine, and synthesized a series of monomeric divalent and trivalent iron and manganese complexes containing metal oxo or hydroxo groups. Dimerization was prohibited by this ligand through the protection of the three bulky *tert*-butyl groups and a rigid H-bonding cavity around the coordination sites housing the oxo or hydroxo ligands.^{15a–d} In the case of the Me₂EBC complexes, dimerization of hydroxo derivatives is prevented by the bulky methyl groups of the tetradenate ligand. This was proven by the synthesis of the corresponding complexes in which the methyl groups were replaced by hydrogen atoms. In their trivalent states, both the iron and manganese complexes of H₂EBC readily formed dimers of the familiar μ -O-bridged kind. Further, manganese(IV/III) dimers were also identified. An X-ray structure proved the μ -O dimeric

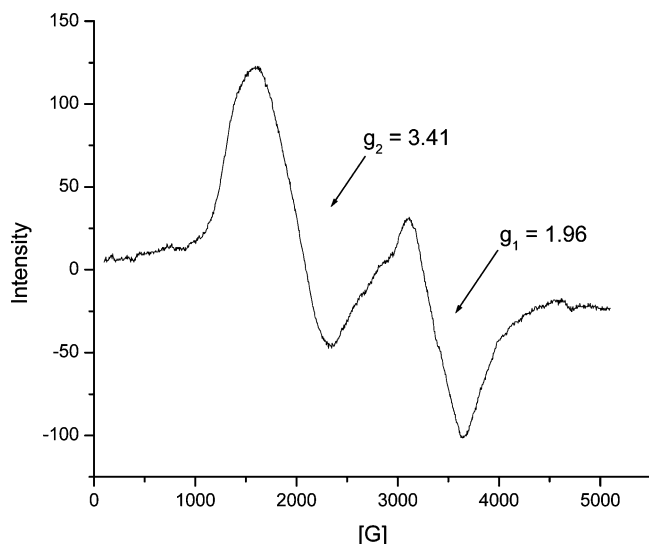


Figure 3. EPR spectrum of $[\text{Mn}^{\text{IV}}(\text{Me}_2\text{EBC})(\text{OH})_2](\text{PF}_6)_2$ in dry acetonitrile at 77 K.

structure for the iron(III) complex,^{11b} while the corresponding dimers of manganese were characterized spectroscopically.^{11e}

Solution Structure of the Mn(IV) Complexes. The EPR spectrum of $[\text{Mn}^{\text{IV}}(\text{Me}_2\text{EBC})(\text{OH})_2](\text{PF}_6)_2$ in dry acetonitrile at 77 K showed two broad resonances at $g = 1.96$ and 3.41 (Figure 3). This spectrum is essentially identical to the EPR reported by Kerschner and co-workers for a manganese(IV) complex containing a N,N,N' -trimethyl-1,4,7-triazacyclononane ligand.¹⁷ Splitting resulting from the nuclear spin of manganese was not observed in either case. The spectrum in Figure 3 is typical of a high-spin d^3 ion with axial symmetry in a strong ligand field and confirms the manganese(IV) oxidation state in $\text{Mn}^{\text{IV}}(\text{Me}_2\text{EBC})(\text{OH})_2^{2+}$.¹⁸ The cyclic voltammogram of $[\text{Mn}^{\text{IV}}(\text{Me}_2\text{EBC})(\text{OH})_2](\text{PF}_6)_2$ in dry acetonitrile is shown in Figure 4, and the redox potentials and peak separations are summarized in Table 3. The cross-bridged macrocyclic ligand stabilizes oxidation states ranging from Mn^{2+} to Mn^{4+} for this manganese complex, as shown by the reversible redox behavior of $\text{Mn}^{\text{IV}}(\text{Me}_2\text{EBC})(\text{OH})_2^{2+}$. From Table 2, one can see that $\text{Mn}^{\text{IV}}(\text{Me}_2\text{EBC})(\text{OH})_2^{2+}$ is a mild oxidant with $\text{Mn}^{4+}/\text{Mn}^{3+}$ redox potential couple of 0.765 V. Another redox couple with potential of +1.013 V is small in amplitude compared with the other couples, and the reductive peak is not very clear. This suggests the possibility that small amounts of Mn^{5+} species may be formed in the electrochemical process in acetonitrile but is not conclusive. Experiments designed to generate manganese(V) and confirm its presence failed, uniformly leading to ligand decomposition. The moderate redox potential required to produce $\text{Mn}^{\text{IV}}(\text{Me}_2\text{EBC})(\text{OH})_2^{2+}$ supports the practical observation that the $\text{Mn}^{\text{II}}(\text{Me}_2\text{EBC})^{2+}$ complex is a selective oxidative catalyst with a variety of terminal oxidants.

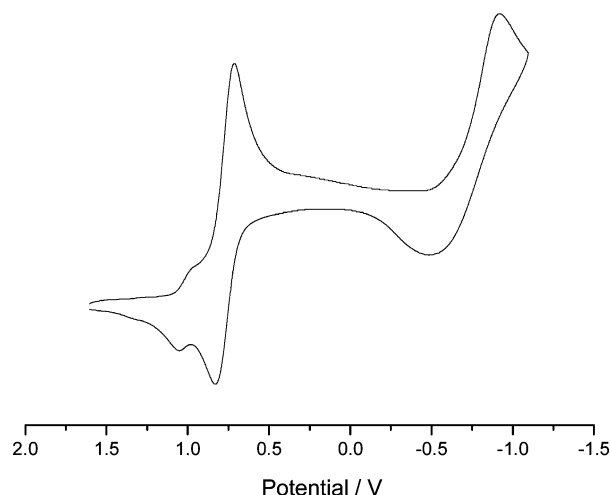


Figure 4. Cyclic voltammogram for $[\text{Mn}^{\text{IV}}(\text{Me}_2\text{EBC})(\text{OH})_2](\text{PF}_6)_2$ in dry acetonitrile.

Table 3. Redox Potentials and Peak Separations for $[\text{Mn}^{\text{IV}}(\text{Me}_2\text{EBC})(\text{OH})_2](\text{PF}_6)_2$ (vs SHE) in Dry Acetonitrile under Nitrogen at 298 K

redox couple	$E_{1/2}$ (V)	$(E_a - E_c)$ (mV)
$\text{Mn}^{5+}/\text{Mn}^{4+}$	+1.013	71
$\text{Mn}^{4+}/\text{Mn}^{3+}$	+0.756	121
$\text{Mn}^{3+}/\text{Mn}^{2+}$	-0.696	388

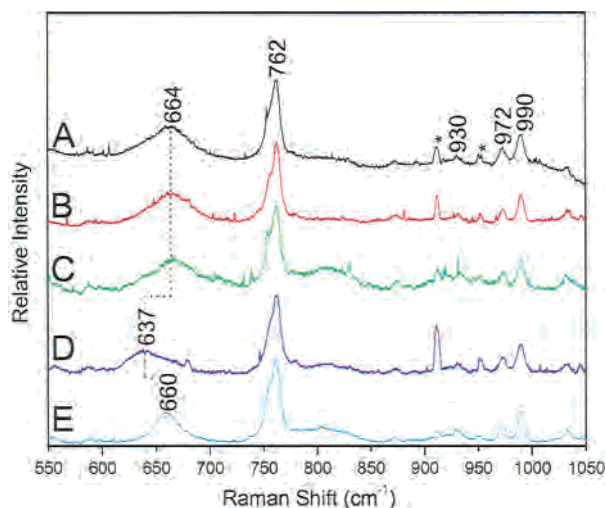


Figure 5. Low-frequency resonance Raman spectra of the oxidized Mn(II)-bridged cyclam complex: (A) Mn(II) and aqueous H_2O_2 , (B) purple solid from oxidized Mn(II) complex,¹⁹ Mn(IV) complex dissolved in H_2O , (C) Mn(II) and aqueous $\text{H}_2^{18}\text{O}_2$ (60 atom %), (D) Mn(II) and H_2O_2 in H_2^{18}O (95 atom %), and (E) Mn(II) and H_2O_2 in D_2O . $\lambda_{\text{exc}} = 413.1$ nm. Laser power = 9 mW. Asterisks indicate Kr plasma lines.

Raman spectral studies were conducted on manganese(IV) species prepared in solution. Oxidation of the corresponding Mn(II) complex, $\text{Mn}^{\text{II}}(\text{Me}_2\text{EBC})\text{Cl}_2$, was achieved by addition of a 10-fold excess of aqueous H_2O_2 to an aqueous solution of Mn(II). Figure 5 shows low-frequency resonance Raman (rR) spectra of the purple oxidized Mn complex under the conditions described in the figure legend. Sample integrity and stability under laser irradiation were judged by the UV-vis absorbance spectrum of the purple oxidized complex. The spectra of the samples were identical to that obtained from the isolated and purified complex. Moreover, the spectrum was unchanged by laser irradiation

(17) Quee-Smith, V. C.; Delpizzo, L.; Jureller, S. H.; Kerschner, J. L. *Inorg. Chem.* **1996**, *35*, 6461.

(18) (a) Fallis, I. A.; Farrugia, L. J.; Macdonald, N. M.; Peacock, R. D. *J. Chem. Soc., Dalton Trans.* **1993**, 2759. (b) Kessissoglou, D. P.; Li, X.; Butler, W. M.; Pecoraro, V. L. *Inorg. Chem.* **1987**, *26*, 2487. (c) Chan, M. K.; Armstrong, W. H. *Inorg. Chem.* **1989**, *28*, 3777. (d) Chandra, S. K.; Chakravorty, A. *Inorg. Chem.* **1992**, *31*, 760.

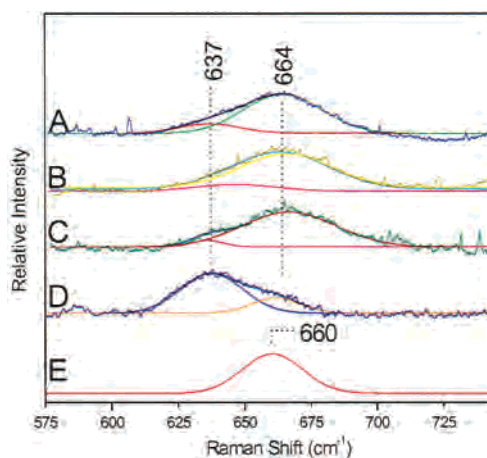
Table 4. High-Valent Mn–O Stretching Frequencies

high-valent Mn species	$\nu_{\text{Mn-O}}$ frequency (cm ⁻¹)	isotope shift
Mn ^V =O ²¹	979 (¹⁸ O = 947 cm ⁻¹)	-32 cm ⁻¹
Mn ^{IV} =O(TPP) ²²	757 (¹⁸ O = 726 cm ⁻¹)	-31 cm ⁻¹
Mn ^{IV} =O(TMP) ²³	754 (¹⁸ O = 722 cm ⁻¹)	-32 cm ⁻¹
Mn ^{IV} -OH(HRP) ²⁴	620 (¹⁸ O = 585 cm ⁻¹)	-35 cm ⁻¹
	(² H = 602 cm ⁻¹)	-18 cm ⁻¹
Mn ^{IV} -OH (bridged cyclam)	664 (¹⁸ O = 637 cm ⁻¹)	-27 cm ⁻¹
	(² H = 660 cm ⁻¹)	-4 cm ⁻¹

of the sample during the resonance Raman experiment. Raman scattering was excited at 413.1 nm where the Mn(II) starting complex has very low extinction. Thus, scattering by the starting material is not resonance enhanced at this wavelength. The 664 cm⁻¹ band shifts to lower frequency when the oxidation reaction is carried out in H₂¹⁸O or in the presence of ²H₂O. These shifts support assignment of the 664 cm⁻¹ band to a Mn^{IV}-OH stretching vibration ($\nu_{\text{Mn(IV)-OH}}$) and argue that the Mn^{IV}-OH coordination observed in the solid state by X-ray crystallography persists in solution. When Mn(II) was oxidized using H₂¹⁸O₂, there was no apparent shift of the 664 cm⁻¹ band. The $\nu_{\text{Mn(IV)-OH}}$ band is quite broad, consistent with structural inhomogeneity in solution. This breadth may be rationalized in terms of multiple H-bond conformations involving the cis hydroxo ligands. Interestingly, this band sharpens in D₂O, suggesting a deuterium isotope effect on the distribution of Mn^{IV}(OD)₂ conformers. The 27 cm⁻¹ downshift was only observed when the oxidation was carried out in H₂¹⁸O. Hence, the oxygen atom of the bound hydroxide comes from water, and the rapid oxygen exchange between the terminal hydroxo ligand of the manganese(IV) complex and water, H₂¹⁸O, has been confirmed through mass spectral studies and reported elsewhere.¹⁹ Although the 762 cm⁻¹ band is in the frequency range expected for a manganyl stretching mode ($\nu_{\text{Mn(IV)=O}}$), its frequency is insensitive to oxidation with H₂¹⁸O₂ or equilibration with H₂¹⁸O. Hence, this band is not assigned to a $\nu_{\text{Mn(IV)=O}}$ mode. This result is consistent with the X-ray structure of [Mn^{IV}(Me₂EBC)(OH)₂](PF₆)₂·H₂O, which revealed the absence of oxo ligands.

Table 4 presents the Mn–O stretching frequencies and their respective isotope shifts for a variety of high-valent oxo and hydroxo manganese complexes. Together with the rR data in Figure 5, these frequencies and isotope shifts support assignment of the Mn^{IV}(OH)₂²⁺ moiety. Taken together, the rR spectra, the *S* = 3/2 EPR spectrum, the improbability that an Mn(V)=O unit would remain protonated at neutral pH, the crystal structure, and the elemental composition are consistent in their support of the *cis*-Mn^{IV}(OH)₂²⁺ unit in both solution and the solid state.

Peak fitting (Figure 6) indicates the presence of two bands within the 664 cm⁻¹ envelope, one at 664 and the other at 637 cm⁻¹ (Figure 6A–D). Oxidation by H₂O₂ in D₂O shifts the 664 cm⁻¹ band to 660 cm⁻¹ (Figure 6E).^{23,24} Although

**Figure 6.** Peak fits of the ²H and ¹⁸O sensitive region of the low-frequency rR spectrum. Experimental conditions were as described for Figure 5.

this shift is small relative to that listed in Table 3 for Mn–HRP, substitution of the proton on coordinated hydroxide ligands by deuterium can cause either upshifts or downshifts in the M–O stretching frequency, depending upon the extent of coupling between the M–O stretch and the M–O–H bend. Oxidation by H₂O₂ in H₂¹⁸O shifts the 664 cm⁻¹ band to 637 cm⁻¹ (Figure 6D). The reason for the disappearance of the 637 cm⁻¹ band in D₂O is unclear. It could be an overtone or combination band comprising a deuterium-sensitive fundamental.

The remarkable kinetic stability of Me₂EBC complexes has been demonstrated in earlier studies with a variety of metal ions, including manganese(II).^{10c,11a,25} This stability facilitates detailed study of the complexes under a variety of conditions, including solution studies over a broad pH range. Thus, the stability of [Mn^{IV}(Me₂EBC)(OH)₂](PF₆)₂ facilitates measurement of the acid–base properties of the OH groups by pH titration in aqueous solution. The titration curve shows two endpoints (Figure 7), and the data were fit using the program HYPERQUAD. The p*K*_{a1} associated with the first proton dissociation from Mn^{IV}(Me₂EBC)(OH)₂²⁺ is 6.86(4), indicating that the dihydroxo complex is the main species in aqueous solutions having pH values below ~7, whereas in neutral and basic media, Mn^{IV}(Me₂EBC)(O)(OH)⁺ becomes the main species (eq 1). This is fully consistent with the results of resonance Raman studies in which the purple species in the oxidized weakly acidic solution was assigned a structure containing the Mn^{IV}(OH)₂ function. The data defining the second endpoint at ~10 conforms best to an unexpected dimer formation, rather than simple deprotonation of the mononuclear complex Mn^{IV}(Me₂EBC)(O)(OH)⁺ (eq 2). This is consistent with mass spectral data for Mn^{IV}(Me₂EBC)(OH)₂²⁺ in base, which showed small amounts of an unidentified dimer (*vide infra*).

(19) Buchalova, M.; Busch, D. H. Unpublished results.

(20) Yin, G.; Buchalova, M.; Danby, A. M.; Perkins, J.; Kitko, D.; Carter, J. D.; Scheper, W. M.; Busch, D. H. *J. Am. Chem. Soc.* **2005**, *127*, 17170.(21) Collins, T. J.; Powell, R. D.; Slebodnick, C.; Uffelman, E. S. *J. Am. Chem. Soc.* **1990**, *112*, 899.(22) Czernuszewicz, R. S.; Su, Y. O.; Stern, M. K.; Macor, K. A.; Kim, D.; Groves, G. T.; Spiro, T. G. *J. Am. Chem. Soc.* **1988**, *110*, 4158.(23) Makino, R.; Uno, T.; Nishimura, Y.; Iizuka, T.; Tsuboi, M.; Ishimura, Y. *J. Biol. Chem.* **1986**, *261*, 8376.(24) Shiemke, A. K.; Loehr, T. M.; Sanders-Loehr, J. *J. Am. Chem. Soc.* **1986**, *108*, 2437.(25) (a) Cagginess, D. K.; Margerum, D. W. *J. Am. Chem. Soc.* **1970**, *92*, 2151. (b) Hubin, T. J.; McCormick, J. M.; Collinson, S. R.; Alcock, N. W.; Busch, D. H. *J. Chem. Soc., Chem. Comm.* **1998**, 1675.

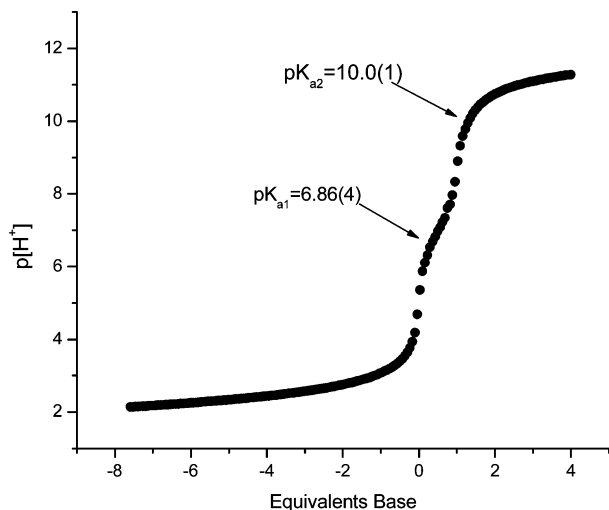
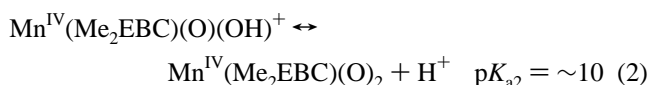
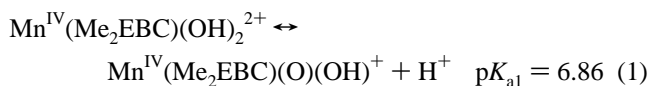


Figure 7. Titration curve for $[\text{Mn}^{\text{IV}}(\text{Me}_2\text{EBC})(\text{OH})_2](\text{PF}_6)_2$ with pH^+ plotted against equivalents of base and constants calculated per mole of $[\text{Mn}^{\text{IV}}(\text{Me}_2\text{EBC})(\text{OH})_2](\text{PF}_6)_2$.

However, it must be emphasized that the Mn^{IV} complex is unstable in basic media and that the contribution of that factor to the results at high pH is not understood.



Stability Limitations of the Tetravalent Complex. The relatively high manganese oxidation state in $\text{Mn}^{\text{IV}}(\text{Me}_2\text{EBC})(\text{OH})_2^{2+}$ is accompanied by limited stability even at room temperature. When it stands in air, the purple color at the surface of dry $[\text{Mn}^{\text{IV}}(\text{Me}_2\text{EBC})(\text{OH})_2](\text{PF}_6)_2$ powder turns orange in a few days, and the electronic spectrum of the resulting orange powder, when dissolved in aqueous solution, corresponds to that of the trivalent $\text{Mn}^{\text{III}}(\text{Me}_2\text{EBC})^{3+}$ species.

The UV-vis spectrum of $\text{Mn}^{\text{IV}}(\text{Me}_2\text{EBC})(\text{OH})_2^{2+}$ in aqueous solution shows that the complex remains stable for a few days in weakly acidic to neutral solution, while in a solution with $\text{pH} < 2$, $\text{Mn}^{\text{IV}}(\text{Me}_2\text{EBC})(\text{OH})_2^{2+}$ gradually degrades to $\text{Mn}^{\text{III}}(\text{Me}_2\text{EBC})^{3+}$ on the time scale of days. When aqueous $\text{Mn}^{\text{IV}}(\text{Me}_2\text{EBC})(\text{OH})_2^{2+}$ was kept for weeks at very low pH (in $\sim 0.4 \text{ M HCl}$), no $\text{Mn}^{\text{III}}(\text{Me}_2\text{EBC})^{3+}$ species could be detected in the electronic spectra, and crystals of free ligand were eventually isolated and identified by X-ray diffraction studies. The mass spectra of the resulting solution displayed the presence of $\text{Mn}^{\text{II}}(\text{MeEBC})(\text{H}_2\text{O})(\text{OH})^+$ along with high concentrations of free ligand but showed no significant evidence (ms peaks) of ligand damage (see Supporting Information). These results reveal complete separation of the ligand from the metal ion in strongly acidic solutions but little or no oxidation of the ligand. Also, the colorless solution indicates that the free manganese ion is reduced to the divalent state under strongly acidic conditions.

In basic media, complexes containing the $\text{Mn}^{\text{IV}}(\text{Me}_2\text{EBC})^{4+}$ unit are unstable. They gradually convert to $\text{Mn}^{\text{II}}(\text{Me}_2\text{EBC})^{2+}$ derivatives,

and the latter are stable for long periods of time. Interestingly, a reversible disproportionation is observed when the manganese(III) complex is present in acid solution. Upon adjustment of the pH value of a basic solution containing the previously synthesized and characterized manganese(III) complex to $\text{pH} < 7$ (i.e., $\text{pH} \sim 5$), the yellow color of the manganese(III) compound immediately changes to the purple color of the manganese(IV) derivative. Furthermore, the color can be shifted back to yellow by again adjusting the pH of solution to $\text{pH} > 7$. This process can be rapidly repeated many times with the same solution. A reasonable explanation for this phenomenon is the existence of an equilibrium between manganese(III), in basic media, and a mixture of manganese(II) and manganese(IV), formed by disproportionation in acidic media (eq 3).



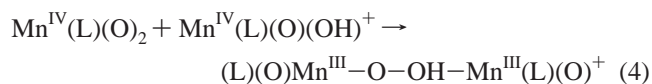
In contrast to the behavior just described for the manganese(III) complex, the corresponding manganese(IV) complex suffers some irreversible degradation in basic media. During the degradation of the $\text{Mn}^{\text{IV}}(\text{Me}_2\text{EBC})^{4+}$ species in base, no dioxygen was detected by an oxygen electrode (estimated detection limit, $\pm 3 \times 10^{-6} \text{ M}$). With high initial concentrations of complex, quantitative analysis of the degraded solution of $\text{Mn}^{\text{IV}}(\text{Me}_2\text{EBC})(\text{O})(\text{OH})^+$ yielded $\text{Mn}^{\text{III}}(\text{Me}_2\text{EBC})(\text{OH})_2^+$ in a reproducible $88 \pm 1\%$ yield; $8.9 \pm 0.4\%$ of the starting complex was recovered, from the same samples, as dark precipitates (calculated as MnO_2) which were not combustible in air. By comparison with a standard mass spectrum of $\text{Mn}^{\text{III}}(\text{Me}_2\text{EBC})(\text{OH})_2^+$, the resulting mass spectra of the degraded solution also displayed substantial “trash” peaks with low mass, including $m/z = 243, 229, 200,$ and 183 , indicating ligand destruction (m/z of HL^+ , 255). Furthermore, this sequence of trash peaks suggests the successive loss of single carbon or single nitrogen units from the damaged ligand. Further, no significant free ligand peak was observed in this mass spectrum. In addition, this mass spectrum showed a very weak peak of high mass (e.g., $m/z = 656$), which hints at the existence of some dimeric complex (m/z of the monomer, $\text{Mn}^{\text{IV}}(\text{Me}_2\text{EBC})(\text{O})(\text{OH})^+$, = 342). This weak high mass peak directed attention toward the acid-base titration results in which the pH data defining $\text{p}K_{\text{a}2}$ (~ 10) indicate the formation of a dimer during the titration process. As stated above, trivalent and tetravalent manganese complexes show a great proclivity to form various dimeric or trimeric linkages through a variety of bridging groups, including oxo and hydroxo groups.²⁶ Also as discussed earlier, the *N*-methyl groups of $\text{Mn}^{\text{IV}}(\text{Me}_2\text{EBC})(\text{O})(\text{OH})^+$ that project above and below the plane containing the manganese and the two hydroxyl groups obviate dimer formation by M–O–M bridging. The $m/z = 656$ peak

(26) (a) Cooper, S. R.; Dismukes, G. C.; Klein, M. P.; Calvin, M. *J. Am. Chem. Soc.* **1978**, *100*, 7248. (b) Arif, A. M.; Jones, R. A.; Schwab, S. T. *J. Organomet. Chem.* **1986**, *307*, 219. (c) Bashkin, J. S.; Chang, H. R.; Streib, W. E.; Huffman, J. C.; Hendrickson, D. N.; Christou, G. *J. Am. Chem. Soc.* **1987**, *109*, 6502. (d) Chen, B.; Chen, K. *Polyhedron* **1989**, *8*, 1029. (e) Banerjee, S.; Choudhury, U. R.; Banerjee, R.; Mukhopadhyay, S. *J. Chem. Soc., Dalton Trans.* **2002**, 2047.

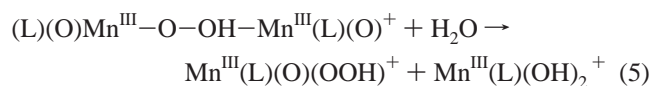
observed in the mass spectrum of $\text{Mn}^{\text{IV}}(\text{Me}_2\text{EBC})(\text{O})(\text{OH})^+$ corresponds roughly to the composition that would result from replacing a methyl group with a hydrogen atom, while retaining both hydroxo and oxo ligands on each monomeric complex. Such a metal complex might more easily undergo dimerization via $\text{Mn}-\text{O}-\text{Mn}$ links. Unfortunately, the results of the accurate mass determination do not support this model: calculated $m/z = 656.3343$ versus accurate $m/z = 656.1129$ and 656.1148 .

The instability of the manganese(IV) species at high pH is important because it represents a limit to the oxidation chemistry of the manganese complexes of bridged cyclam ligands. Further the stoichiometry of the associated degradation process implies total destruction of $8.9 \pm 0.4\%$ of the ligands in the starting materials to produce $88 \pm 1\%$ of the pure manganese(III) complex. The instability can be attributed to the *cisoid* pair of dinegative oxo ligands in the fully deprotonated complex, $\text{Mn}^{\text{IV}}(\text{Me}_2\text{EBC})(\text{O})_2$, for a range of possible reasons and with a variety of possible consequences,²⁷ including redox pathways reminiscent of the roles of manganese in natural products, such as Photosystem II.^{3,28} Pairs of manganese atoms are known to facilitate the formation and dissociation of oxygen–oxygen bonds, an obvious route to dimerization that could accompany final deprotonation of $\text{Mn}^{\text{IV}}(\text{Me}_2\text{EBC})(\text{O})(\text{OH})^+$ in strong base. The pseudo-octahedral dioxo complex, $\text{Mn}^{\text{IV}}(\text{Me}_2\text{EBC})(\text{O})_2$, may present an unusual, strongly oxidizing oxygen atom to the OH group of a still protonated $\text{Mn}^{\text{IV}}(\text{Me}_2\text{EBC})(\text{O})(\text{OH})^+$ cation. The formation of an oxygen–oxygen bond would then produce a dimer, linked by a peroxide bridge.²⁹

According to this model, the dimer is formed as shown in eq 4.



In aqueous media, such a hydroperoxide-bridged dimeric complex would be expected to exist in equilibrium with its simple aquation products, as shown in eq 5.



The hydroperoxide complex formed in the reaction depicted by eq 4 has a molecular structure well suited to

(27) Two alternate possibilities are the following: (1) Given the pseudo-octahedral structure of the coordination sphere of the manganese(IV) ion, the strong repulsion between two neighboring dinegative ligands may not be satisfied by the ability of the central atom to accept double-donor bonding from the oxide ions, and this inherent instability could lead to intramolecular redox of a well know variety in which, for example, the methylamine linkage is oxidized to a radical by internal electron transfer from nitrogen to the metal ion. Thereafter events parallel to those in Figure S1, Supporting Information would follow. (2) The tendency for high valent central atoms to reduce their coordination numbers as the number of proton-free oxide ligands bound to them increases is well-known. This could lead to dissociation of a nitrogen donor from the manganese(IV), and such an intermediate structure could be subject to further oxidation reactions, again paralleling events shown in Figure S1, Supporting Information.

(28) Hoganson, C. W.; Babcock, G. T. *Science* **1997**, *277*, 1953.

intramolecular self-destruction. A simplified and idealized model for the self-destruction of $\text{Mn}^{\text{IV}}(\text{Me}_2\text{EBC})(\text{O})_2$ is presented in the Supporting Information.

Conclusions

In summary, we have synthesized and characterized a novel manganese(IV) complex of a cross-bridged cyclam ligand, $[\text{Mn}^{\text{IV}}(\text{Me}_2\text{EBC})(\text{OH})_2](\text{PF}_6)_2$. The complex has been characterized as a monomer with the unusual feature that it has a *cisoid* pair of monodentate hydroxo ligands in both the solid state (X-ray structure) and in solution (resonance Raman). The tetravalent oxidation state has been established by X-ray, EPR, electrochemistry studies, and $\text{p}K_{\text{a}}$ values. pH titration of aqueous solutions of $\text{Mn}^{\text{IV}}(\text{Me}_2\text{EBC})(\text{OH})_2^{2+}$ show two acid–base equilibria with $\text{p}K_{\text{a}1} = 6.86$ and $\text{p}K_{\text{a}2} = \sim 10$, the latter apparently being associated with dimer formation. In weakly acidic solutions, $\text{Mn}^{\text{IV}}(\text{Me}_2\text{EBC})(\text{OH})_2^{2+}$ is the dominant species. As the pH approaches 7, $\text{Mn}^{\text{IV}}(\text{Me}_2\text{EBC})(\text{O})(\text{OH})^{2+}$ becomes dominant, and above pH 10, the complex becomes fully deprotonated $\text{Mn}^{\text{IV}}(\text{Me}_2\text{EBC})(\text{O})_2$; the latter species is unstable, decomposing spontaneously. The positioning of the *N*-methyl groups on the cross-bridged cyclam ligand, prevents dimerization of this manganese(IV) complex through common one-atom μ -oxo bridges. Stabilized by the terminal dihydroxo ligands, this manganese(IV) complex displays a moderate redox potential of $+0.756$ V vs SHE for the manganese(IV/III) couple, and it is relatively stable in weakly acidic and neutral aqueous solution and also in the solid state in the presence of air at room temperature. However, this manganese(IV) compound is unstable in base and gradually degrades to the manganese(III) derivative, $\text{Mn}^{\text{III}}(\text{Me}_2\text{EBC})^{3+}$, with a yield of $\sim 88 \pm 1\%$. The decomposition process is complicated and involves ligand destruction and formation of the metal oxides. In very strong acid solution, the complex is destroyed and the ligand can be reclaimed intact. To our knowledge, this manganese(IV) compound is the first isolated and well-characterized manganese(IV) complex with terminal hydroxo ligands. Since high oxidation state manganese moieties with terminal hydroxo ligands are generally believed to exist in the oxygen-evolving complex (OEC) of Photosystem II, $\text{Mn}^{\text{IV}}(\text{Me}_2\text{EBC})(\text{OH})_2^{2+}$ may serve in future studies of the oxygen-evolving mechanism. Certainly, this manganese(IV) complex provides a convenient reactant for investigations aimed at understanding the catalytic reactions mediated by these manganese catalysts, including processes such as hydrogen abstraction and oxygen-atom transfer.

(29) This rationalization is attractive for three reasons. (1) It is consistent with the ability of manganese systems to facilitate O–O bond formation and breakage. (2) The resulting 2-atom bridge would be long enough to overcome the inherent steric restrictions of pseudo-octahedral derivatives of Me_2EBC that prevent bridge formation (repulsion between the methyl groups of the different ligands). (3) The proposed peroxide-bridged species provides an appealing basis for rationalizing the stoichiometry observed for the conversion of $\text{Mn}^{\text{IV}}(\text{Me}_2\text{EBC})(\text{O})_2$ into $[\text{Mn}^{\text{III}}(\text{Me}_2\text{EBC})(\text{OH})_2]\text{PF}_6$ in basic media.

Cross-Bridged Cyclam Manganese(IV) Complex

Acknowledgment. Support by the Procter and Gamble Company is deeply appreciated, and we also thank the National Science Foundation Engineering Research Center Grant (EEC-0310689) for partial support. At KU, MS analyses of the manganese(IV) complex under various conditions were performed by R. C. Drake, and the crystal structure was determined by Douglas Powell.

Supporting Information Available: Detailed crystal structure data for the manganese(IV) complex, model for the self-destruction of the manganese(IV) complex in base, mass spectra of manganese(IV) complex in 0.4 M HCl, and mass spectra of manganese(IV) complex in basic solution. This material is available free of charge via the Internet at <http://pubs.acs.org>.

IC0521123